THE JOURNAL OF BIOLOGICAL CHEMISTRY VOL. 281, NO. 36, pp. 26734–26744, September 8, 2006
Printed in the U.S.A.

Probing Active Site Chemistry in SHV β-Lactamase Variants at Ambler Position 244

*UNDERSTANDING UNIQUE PROPERTIES OF INHIBITOR RESISTANCE**

Received for publication, April 5, 2006, and in revised form, June 12, 2006 Published, JBC Papers in Press, June 27, 2006, DOI 10.1074/jbc.M603222200

Jodi M. Thomson[‡1], Anne M. Distler[‡], Fabio Prati[§2], and Robert A. Bonomo[‡¶3]

From the [‡]Department of Pharmacology, Case Western Reserve University School of Medicine, Cleveland, Ohio 44106, the [§]Department of Chemistry, University of Modena, 41100 Modena, Italy, and the [¶]Louis Stokes Cleveland of Veterans Affairs Medical Center, Cleveland, Ohio 44106

Inhibitor-resistant class A β-lactamases are an emerging threat to the use of β-lactam/β-lactamase inhibitor combinations (*e.g.* amoxicillin/clavulanate) in the treatment of serious bacterial infections. In the TEM family of Class A β-lactamases, single amino acid substitutions at Arg-244 confer resistance to clavulanate inactivation. To understand the amino acid sequence requirements in class A β-lactamases that confer resistance to clavulanate, we performed site-saturation mutagenesis of Arg-244 in SHV-1, a related class A β-lactamase found in *Klebsiella pneumoniae*. Twelve SHV enzymes with amino acid substitutions at Arg-244 resulted in significant increases in minimal inhibitory concentrations to ampicillin/clavulanate when expressed in *Escherichia coli*. Kinetic analyses of SHV-1, R244S, R244Q, R244L, and R244E β-lactamases revealed that the main determinant of clavulanate resistance was reduced inhibitor affinity. In contrast to studies in the highly similar TEM enzyme, we observed increases in clavulanate k_{inact} for all mutants. Electrospray ionization mass spectrometry of clavulanate inhibited SHV-1 and R244S showed nearly identical mass adducts, arguing against a difference in the inactivation mechanism. Testing a wide range of substrates with C_{3-4} carboxylates in different stereochemical orientations, we observed impaired affinity for all substrates among inhibitor resistant variants. Lastly, we synthesized two boronic acid transition state analogs that mimic cephalothin and found substitutions at Arg-244 markedly affect both the affinity and kinetics of binding to the chiral, deacylation transition state inhibitor. These data define a role for Arg-244 in substrate and inhibitor binding in the SHV β-lactamase.

β-Lactams have been the cornerstone of antibacterial chemotherapy since the introduction of penicillin. Although this family of antibiotics now contains numerous classes (penicillins, cephalosporins, and carbapenems, see Fig. 1), their use is threatened by the expansion and spread of β-lactamase enzymes (1). These bacterial enzymes hydrolyze β-lactam antibiotics before reaching their target, the penicillin-binding proteins. In an effort to retain the utility of several generations of life-saving β-lactam antibiotics, β-lactamase inhibitors (clavulanate, sulbactam, and tazobactam) have been developed. These mechanism-based inhibitors are β-lactam compounds that experience multistep reactions within the active site of β-lactamase enzymes (2–4). Typically the inhibitors lack antimicrobial activity and are formulated with a β-lactam antibiotic to act as shields against β-lactamase enzymes. This allows the β-lactam to bypass the β-lactamase and inactivate the penicillin binding proteins.

Unfortunately, inhibitor-resistant class A β-lactamases are emerging in the clinic and undermining the use of β-lactam/β-lactamase inhibitor therapy (5–7). Interest has been renewed in the discovery of novel β-lactamase inactivators to circumvent these inhibitor-resistant enzymes (8–11). In this context, detailed analyses of enzymes resistant to the inhibitors are needed to minimize cross-resistance and guide discovery.

Both S130G and M69I mutations conferring inhibitor resistance have been described in TEM[4] and SHV β-lactamase families (enzymes with 68% amino acid identity).[5] A notable exception, however, is the absence of clinical variants with substitutions at Ambler[6] position Arg-244 in SHV compared with TEM. Arg-244 is situated at the periphery of the active site pocket in the B4 β-strand (13). Although 15 distinct inhibitor-resistant TEM enzymes have been reported with substitutions at this residue, mutations at Arg-244 in SHV have not been described in clinical isolates.[5]

The mechanism of clavulanate resistance resulting from substitutions at position 244 in TEM was previously examined (14–16). Structural and computational studies of TEM-1 show

* This work was supported in part by the Veterans Affairs Medical Center Merit Review Program and National Institutes of Health (NIH) Grant 1R01 A1063517-01. The costs of publication of this article were defrayed in part by the payment of page charges. This article must therefore be hereby marked "*advertisement*" in accordance with 18 U.S.C. Section 1734 solely to indicate this fact.
[1] Supported by NIH Grant T32 GM07250 and the Case Medical Scientist Training Program.
[2] Supported by the Fondazione Cassa di Risparmio di Modena.
[3] To whom correspondence should be addressed: Division of Research Service, Louis Stokes Cleveland Veterans Affairs Medical Center, 10701 East Blvd., Cleveland, OH 44106. Tel.: 216-791-3800 (ext. 4399); Fax: 216-231-3482; E-mail: robert.bonomo@med.va.gov.

[4] The abbreviations used are: TEM, Class A β-lactamase named after the patient (Temoneira) from whom the first β-lactamase was isolated; SHV, Class A β-lactamase named after the property sulfhydryl reagent variable; MIC, minimal inhibitory concentration; TMS, tetramethyl silane; δ, chemical shifts; s, singlet; d, doublet; t, triplet; q, quartet; m, multiplet; br, broad signal; *J*, coupling constants; EI, electron impact; EIMS, electron impact mass spectrometry; THF, tetrahydrofuran; mp, melting point.
[5] G. A. Jacoby and K. Bush (2006) www.lahey.org/studies/webt.asp.
[6] The Ambler numbering system was developed to standardize the amino acid positions in Class A β-lactamases with different chain lengths.

that Arg-244 coordinates a water molecule with the backbone carbonyl of Val-216 (10, 15, 16). This water molecule is postulated to play a key role in inhibitor affinity and provide the proton source essential for terminal inactivation of the enzyme (Fig. 2) (16). In addition, the guanidinium group of Arg-244 contributes directly to substrate affinity through hydrogen bonding with the conserved β-lactam carboxylate (10) (Figs. 1 and 2). Inhibitor-resistant TEM β-lactamases with substitutions at Arg-244 exhibit reduced rates of inactivation (k_{inact}) as well as diminished affinity for clavulanate and substrates (14, 16).

We hypothesized that the absence of mutations identified in SHV at this position, despite heavy clinical drug pressure, is an indication of important differences in active site chemistry between the two highly similar enzymes. To test this hypothesis, we investigated the effects of multiple amino acid substitutions by site-saturation mutagenesis and characterized select SHV β-lactamases by steady-state kinetics. To compare the nature of the intermediates in the inactivation process, we incubated SHV-1 and SHV R244S, a clavulanate-resistant variant, with clavulanate and resolved the adducts by electrospray ionization mass spectrometry. In addition, we studied the inhibition of several SHV β-lactamase variants at position 244 using two boronic acid transition state analogs that are chemically related to the antibiotic cephalothin (Fig. 1). Our results reveal mechanistic differences in clavulanate inactivation between SHV-1 and TEM-1 and suggest a new role for Arg-244 in SHV.

EXPERIMENTAL PROCEDURES

Plasmids and Mutagenesis—bla_{SHV-1}, subcloned into phagemid vector pBC SK(−) (Stratagene, La Jolla, CA) and maintained in ElectroMAX™ DH10B™ $T1^R$ cells (Invitrogen) as previously described (17) served as the template for all mutagenesis described herein. Site-saturation mutagenesis was performed on the bla_{SHV-1} construct using the QuikChange® II site-directed mutagenesis kit (Stratagene) and primers degenerate at Ambler position 244. Two microliters of the mutagenesis reaction was transformed into *Escherichia coli* DH10B electrocompetent cells (Invitrogen) and plated onto Luria-Bertani (LB) agar plates using chloramphenicol (Sigma-Aldrich, 20 μg/ml) for selection. One hundred colonies were screened for mutations at amino acid position 244 by DNA sequencing with an ALF Express™ automated DNA sequencer (GE, Piscataway, NJ). The Thermo Sequenase™ fluorescence-labeled primer cycle sequencing kit was used according to the protocol provided. Special attention was given to selecting mutants with the most common codon usage in SHV-1.

Because the R244K, -Met, and -Phe mutants were not obtained in the initial screen, $bla_{SHV-1(R244K)}$, $bla_{SHV-1(R244M)}$, and $bla_{SHV-1(R244F)}$ were constructed by site-directed mutagenesis, using specific mutagenic oligonucleotides as previously described (18). DNA sequencing confirmed the presence of the mutated codons as described above.

Immunoblots—*E. coli* DH10B cells were grown to A_{600} = 0.8 and frozen. Twenty microliters of each culture was lysed by 10-min incubation at 100 °C in SDS loading dye buffer. Immunoblots were performed with an anti-SHV polyclonal antibody to confirm expression of full-length protein from all 20 constructs as previously described (18).

Antibiotic Susceptibility—Minimal inhibitory concentrations (MICs) were determined by the agar dilu-

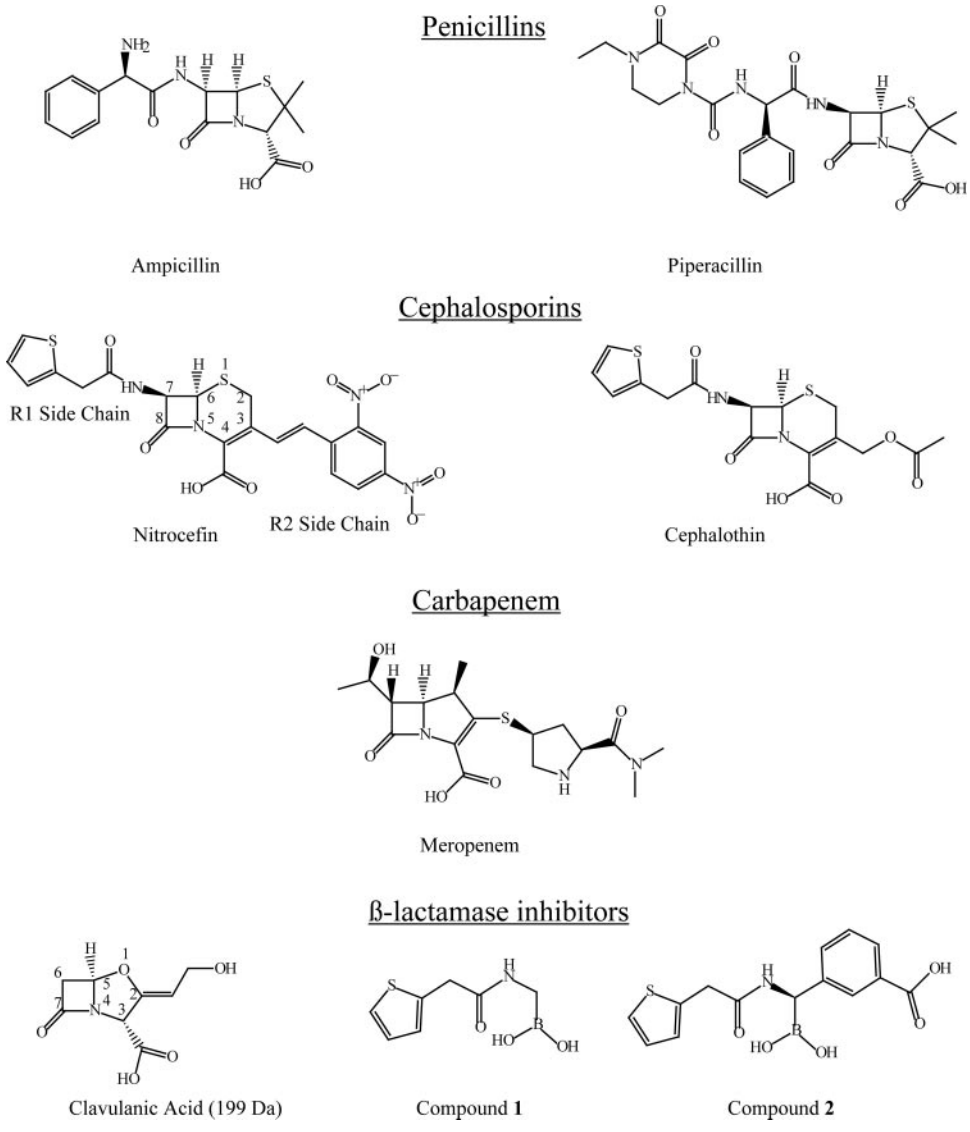

FIGURE 1. **Chemical structures of compounds tested in this study.** The structures of clavulanic acid and nitrocefin are labeled with the accepted ring numbering system.

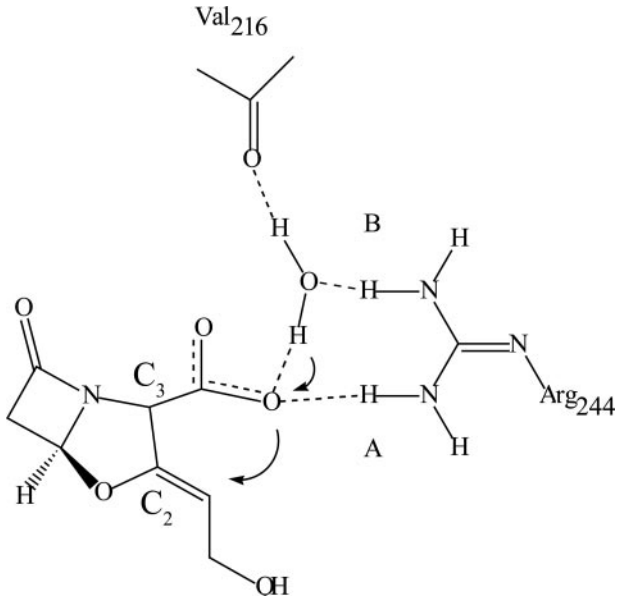

FIGURE 2. **The proposed contribution of Arg-244 to clavulanic acid inactivation of TEM-1.** The guanidinium group of Arg-244 is essential for hydrogen bonding interactions with the C_3 carboxylate of the inhibitor in the active site (*A*) and coordination of a proton donating water molecule essential for the saturation of the double bond of the C_2 constituent (*B*) (16).

tion method, using a Steer's Replicator that delivers 10^4 colony forming units per 10-μl spot. Antibiotics tested include ampicillin, cephalothin, and piperacillin (all from Sigma-Aldrich) and lithium clavulanate (GlaxoSmithKline, Surrey, United Kingdom). Clavulanate susceptibility was determined in the presence of 50 μg/ml ampicillin. MIC values reported are the most frequent number observed (mode) in at least three separate experiments.

Protein Expression and Purification—E. coli DH10B cells containing the $bla_{\text{SHV-1}}$ and $bla_{\text{SHV R244S, R244Q, R244L, and R244E}}$ genes in pBC SK(−) were grown overnight in SOB medium (per liter: 20 g tryptone, 5 g yeast extract, 0.58 g sodium chloride, 0.19 g potassium chloride (Fisher Scientific)) harvested by centrifugation at 4 °C, and frozen. β-Lactamase was liberated using stringent periplasmic fractionation with 40 μg/ml lysozyme and 1 mM EDTA, pH 7.8. Preparative isoelectric focusing was performed with the lysate in a Sephadex granulated gel using ampholines in the pH range of 3.5–10 (Amersham Biosciences) as previously described (19). The protein was eluted and dialyzed with 20 mM diethanolamine buffer, pH 8.5. Protein concentration was assessed by Bio-Rad protein assay with bovine serum albumin standards. Purity of >95% was determined using 10% SDS-PAGE.

Kinetics—Kinetic constants of the β-lactamases chosen for study (SHV-1, R244S, R244Q, R244L, and R244E) were measured by continuous assays at room temperature, 25 °C, using a diode array spectrophotometer (Model 8453, Agilent, Palo Alto, CA). Each assay was performed in 20 mM phosphate-buffered saline at pH 7.4. Measurements were obtained using nitrocefin (BD Biosciences) ($\Delta\epsilon_{482}$ = 17,400 M^{-1} cm^{-1}) and ampicillin ($\Delta\epsilon_{482}$ = −900 M^{-1} cm^{-1}). The kinetic parameters, $V_{\max}$ and K_m, were obtained with non-linear least squares fit of the data (Equation 1) using Origin 7.5®.

$$v = (V_{\max} \times [S])/(K_m + [S]) \quad \text{(Eq. 1)}$$

The dissociation constants of the pre-acylation complex (K_d) were determined by direct competition with the indicator substrate nitrocefin for the β-lactams (cephalothin, piperacillin, and meropenem). The K_i values for the inhibitors (clavulanic acid and the boronic acid inhibitors, compounds **1** and **2**) were also determined by direct competition, because k_{inact}/K_i was $\ll 1$.

Enzyme concentrations for these experiments were adjusted so that an initial rate of nitrocefin hydrolysis between 1 and 1.5 μM/s in the absence of inhibitor was achieved. Final concentrations were 7 nM (SHV-1), 10.5 nM (R244Q), 21 nM (R244S and R244L), and 105 nM (R244E). Nitrocefin concentrations equal to the K_m (Table 2) were used for all experiments, except for R244L in which 200 μM was used due to absorbance limitations. The data were analyzed according to Equation 2 to determine K_i,

$$i = [I]/([I] + K_i(1 + ([S]/K_m))) \quad \text{(Eq. 2)}$$

where i = fraction of enzyme inhibited, $[S]$ = nitrocefin concentration, $[I]$ = inhibitor concentration, and K_m refers to the K_m value of the enzyme for nitrocefin (20).

The first-order rate constant for enzyme and inhibitor complex inactivation, k_{inact}, was measured directly by monitoring the reaction time courses in the presence of clavulanate. A fixed concentration of enzyme and nitrocefin, and increasing concentrations of clavulanate ($[I]$), were used in each assay. The k_{obs} for inactivation was determined graphically by Equation 3,

$$A = v_f \times t + (v_0 - v_f) \times (1 - e^{(-k_{\text{obs}} \times t)})/k_{\text{obs}} + A_0 \quad \text{(Eq. 3)}$$

where A = absorbance, t = time (seconds), v_f = final reaction velocity, v_0 = the initial reaction velocity in the first 5 s, and A_0 = the initial absorbance. Each k_{obs} was plotted *versus* $[I]$ and fit to Equation 4 to determine k_{inact}.

$$k_{\text{obs}} = k_{\text{inact}}[I]/(K_i + [I]) \quad \text{(Eq. 4)}$$

The partitioning of the initial enzyme inhibitor complex between hydrolysis and enzyme inactivation ($k_{\text{cat}}/k_{\text{inact}}$) was obtained in the following manner. First, we incubated increasing amounts of clavulanate with a fixed concentration of β-lactamase in a total volume of 40 μl of 20 mM phosphate-buffered saline, pH 7.4, at room temperature. After 24 h, the sample was added to a 1-ml cuvette containing phosphate-buffered saline and nitrocefin (see above), and initial rates of hydrolysis were assessed. The proportion of clavulanic acid relative to enzyme that resulted in ≥90% inactivation after 24 h was the $k_{\text{cat}}/k_{\text{inact}}$ for the enzyme.

K_i values for the boronic acid compounds were determined as described above. However, because of time-dependant inactivation, enzyme and the boronic acid compound **2** were preincubated for 5 min in phosphate-buffered saline before initiating the reaction with the addition of substrate (10, 21, 22).

Timed inactivation experiments were also performed with clavulanate and the boronic acid compound **2**. To control for the difference in affinities, K_i concentrations of inhibitor were used in each assay. Enzyme and inhibitor were incubated in phosphate-buffered saline for a range of time points before the reaction was initiated by nitrocefin (see above for enzyme and nitrocefin concentrations).

Mass Spectrometry—For intact protein mass spectrometry, 40 μM of SHV-1 or R244S were incubated for 15 min with and without the addition of 40 mM lithium clavulanate. Each reaction was terminated by the addition of 1:10 volume of 1% trifluoroacetic acid and immediately desalted and concentrated using a C_4 ZipTip® (Millipore, Bedford, MA) according to the manufacturer's protocol. Samples were then placed on ice and analyzed within 2 h.

Spectra of the intact SHV-1 and SHV R244S proteins were generated on an Applied Biosystems (Framingham, MA) Q-STAR XL quadrupole-time-of-flight mass spectrometer equipped with a nanospray source. Experiments were performed by diluting the protein sample with acetonitrile/1% formic acid to a concentration of 10 μM. This protein solution was then infused at a rate of 0.5 μl/min, and data were collected for 2 min. Spectra were deconvoluted using the Applied Biosystems (Framingham, MA) Analyst program.

Synthesis of Boronic Acid Inhibitors—^{1}H and ^{13}C NMR spectra were recorded on a Bruker DPX-200 or Avance 400 spectrometer; chemical shifts (δ) are reported in parts per million (ppm) downfield from tetramethyl silane (TMS) as internal standard (s, singlet; d, doublet; t, triplet; q, quartet; m, multiplet; br, broad signal); coupling constants (*J*) are given in hertz. Mass fragmentations were determined on a Finnigan MAT SSQ A mass spectrometer (electron impact (EI), 70 eV). Optical rotations were recorded at 20 °C on a PerkinElmer Life Sciences polarimeter, and specific rotations are given in 10^{-1} deg cm^2 g^{-1}.

All reactions requiring anhydrous conditions were performed under argon using oven-dried glassware. Tetrahydrofuran (THF) was dried according to classic procedures and distilled from sodium/benzophenone before use.

Chromatographic purification of the compounds was accomplished on silica gel (0.05–0.20 mm). 3-Ethoxycarbonylphenylboronic acid and (+)-(1*S*,2*S*,3*R*,5*S*)-pinanediol (enantiomeric excess > 98%) were purchased from Aldrich. Synthesis of the achiral cephalothin boronic acid transition state inhibitor **1** was performed as previously described (23). Enantioselective synthesis of the chiral cephalothin boronic acid transition state inhibitor **2** was performed as follows (Fig. 3) (11).

*(+)-Pinanediol 3-(Ethoxycarbonyl)phenylboronate (+)-(**3**)*—Phenylboronic acid (1,250 g, 6.44 mM) and (+)-pinanediol (1.100 g, 6.44 mM) were dissolved in anhydrous THF (8 ml). The mixture was stirred for 1 h at room temperature and concentrated *in vacuo*. The crude product was purified by chromatography (light petroleum/diethyl ether, 9:1) yielding the ester **3** as a white solid (2.060 g, 97%). The melting point (mp) was 56–58 °C, $[\alpha]_D$: +9.9 (*c* 0.9, $CHCl_3$). Infrared (IR): ν 2984, 2921, and 1718.

^{1}H NMR ($CDCl_3$): δ 0.88 (3H, s, pinanyl CH_3), 1.20 (1H, d, J = 10.2 Hz, pinanyl H_{endo}), 1.31 (3H, s, pinanyl CH_3), 1.39 (3H, t, J = 7.1 Hz, O-CH_2-CH_3), 1.49 (3H, s, pinanyl CH_3), 1.89–2.54 (5H, m, pinanyl protons), 4.38 (2H, q, J = 7.2 Hz, O-CH_2-CH_3), 4.46 (1H, dd, J = 8.6, 1.8, pinanyl C*H*OB), 7.44 (1H, dt, J = 0.5, 7.9 Hz, H_5 arom), 7.98 (1H, dt, J = 7.4, 1.3, H_4 arom), 8.13 (1H, dt, J = 7.8, 1.6, H_6 arom), and 8.48 (1H, br s, H_2 arom).

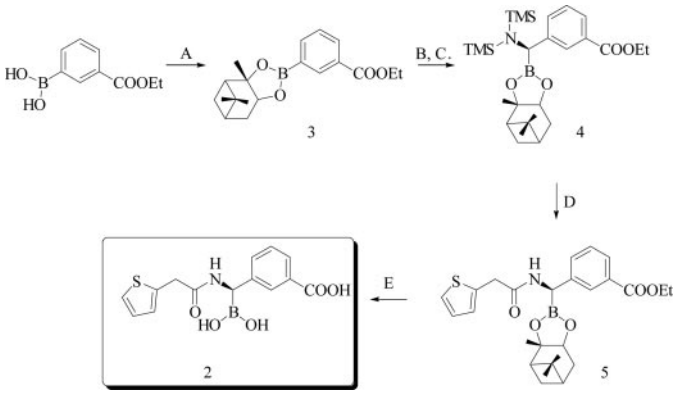

FIGURE 3. **Synthesis of the chiral cephalothin boronic acid transition state inhibitor.** (+)-pinanediol, THF, at room temperature (*A*), (dichloromethyl)-lithium, THF, −100 °C to 0 °C (*B*), lithium bis(trimethylsilyl)amide, THF, −80 °C to room temperature (*C*), 2-thiopheneacetylchloride, 2-thiopheneacetic acid, −80 °C to room temperature (*D*), and aqueous HCl, 3N, 1 h, 100 °C (*E*).

^{13}C NMR ($CDCl_3$): δ 14.4, 24.0, 26.5, 27.1, 28.7, 35.5, 38.2, 39.5, 51.4, 60.9, 78.4, 86.5, 127.7, 130.0, 132.2, 135.8, 139.1, and 166.7 (*C*-B not seen).

Electron impact mass spectrometry (EIMS): *m/z* 328 (44%, M^+), 313 (28%), 287 (25%), 283 (32%), 272 (20%), 259 (base peak), 245 (22%), 232 (76%), 204 (8%), 187 (15%), 177 (11%), 152 (15%), 134 (34%), 131 (20%), 109 (15%), 105 (30%), 96 (33%), 93 (13%), 83 (66%), 77 (15%), 67 (48%), and 55 (25%).

Analytically calculated for $C_{19}H_{25}BO_4$: C, 69.53; H, 7.68. Found: 69.66; H, 7.57.

*(+)-Pinanediol (R)-(3-Ethoxycarbonylphenyl)-(1,1,1,3,3,3-hexamethyldisilazan-2-yl)-methaneboronate (−)-**4***—A solution of methylene chloride (220 μl, 3.4 mM) in THF (4 ml) was cooled at −100 °C and treated with a 2.5 M solution of butyllithium in hexanes (1 ml, 2.56 mM) under an argon flow and magnetic stirring: $LiCHCL_2$ precipitated as a white microcrystalline solid. After 30 min, a solution of the above pinanediol arylboronate (+)-**3** (700 mg, 2.13 mM) in anhydrous THF (6 ml) was added dropwise at −100 °C over a 20-min period. The mixture was gradually allowed to reach 0 °C over 6 h and stirred at this temperature for one additional hour. Thereafter, the solution was cooled at −80 °C, lithium bis(trimethylsilyl)amide (1 M solution in hexane, 2.34 ml, and 2.34 mM) was added, and the reaction mixture was allowed to warm gradually overnight. The resulting solution was partitioned between light petroleum (50 ml) and H_2O (20 ml), and the organic phase was dried over $MgSO_4$, filtered, and concentrated under reduce pressure. The residue was purified by column chromatography (light petroleum/diethyl ether/triethylamine, 70:30:2) affording **4** as a colorless viscous oil (503 mg and 47%), $[\alpha]_D$: −1.7 (*c* 0.4, $CHCl_3$), *de* ≥ 98%. IR: ν 3404, 2936, and 1720.

^{1}H NMR ($CDCl_3$): δ 0.12 (18H, s, TMS), 0.87 (3H, s, pinanyl CH_3), 1.29 (1H, d, J = 10.3 Hz, pinanyl H_{endo}), 1.33 (3H, s, pinanyl CH_3), 1.40 (3H, t, J = 7.2, O-CH_2-CH_3), 1.45 (3H, s, pinanyl CH_3), 1.92–2.46 (5H, m, pinanyl protons), 4.12 (1H, br s, CH-B), 4.37 (3H, m, O-CH_2-CH$_3$ and pinanyl C*H*OB), 7.34 (1H, t, J = 7.7 Hz, H_5 arom), 7.71 (1H, d, J = 7.7 Hz, H_4 arom), 7.84 (1H, d, J = 7.7 Hz, H_6 arom), and 8.24 (1H, m, H_2 arom).

^{13}C NMR ($CDCl_3$): δ 2.4, 14.3, 24.0, 26.5, 27.1, 28.3, 35.4, 38.2, 39.5, 46.6 (br, *C*-B), 51.5, 60.6, 78.6, 86.2, 126.5, 127.5, 128.0, 129.8, 131.1, 145.5, and 167.1.

EIMS: *m/z* 339 (41%, M^+- $N(TMS)_2$), 310 (8%), 294 (19%), 266 (10%), 190 (5%), 163 (100%), 161 (6%), 135 (38%), 119 (69%), 104 (10%), 91 (48%), 77 (19%), and 65 (8%).

Analytically calculated for $C_{26}H_{44}BNO_4Si_2$: C, 62.25; H, 8.84; N, 2.79. Found: C, 62.09; H, 8.99; N, 2.64.

*(+)-Pinanediol (R)-(3-Ethoxycarbonylphenyl)-(2-thiophen-2-yl-acetylamino)methaneboronate (+)-**5***—A solution of 2-thienylacetic acid (149 mg, 1.047 mM) and 2-thienylacetylchloride (130 μl, 1.047 mM) in THF (4 ml) was slowly added to a cooled (−80 °C) solution of (−)-**4** (500 mg, 0.997 mM) in anhydrous THF (10 ml). The resulting solution was allowed to reach room temperature and to react for 15 h; thereafter, the resulting mixture was partitioned between *n*-hexane (50 ml) and H_2O (20 ml), the aqueous phase was repeatedly extracted with *n*-hexane (2 × 20 ml). The collected organic phases were washed with saturated $NaHCO_3$, dried over $MgSO_4$, filtered, and concentrated *in vacuo*. The residue was purified by column chromatography (light petroleum/diethyl ether, 1:9) affording the amide **5** as a white solid (293 mg, 61%). mp, 164–166 °C; $[\alpha]_D$: +15.5 (*c* 0.8, $CHCl_3$), *de* ≥ 98%. IR: *ν* 3173, 2979, 1721, 1612, 1276, 1201, and 1090.

^{1}H NMR ($CDCl_3$): δ 0.7 (3H, s, pinanyl C*H*$_3$), 1.20 (1H, d, *J* = 10.3 Hz, pinanyl H_{endo}), 1.24 (3H, s, pinanyl C*H*$_3$), 1.34 (3H, s, pinanyl C*H*$_3$), 1.39 (3H, t, *J* = 7.1 Hz, OCH_2C*H*$_3$), 1.47–2.5 (5H, m, pinanyl protons), 4.00 (2H, s, CH_2-CO), 4.12 (1H, d, *J* = 2.0 Hz, C*H*-B), 4.21 (1H, dd, *J* = 8.6, 2.2 Hz, pinanyl C*H*OB), 4.37 (2H, q, *J* = 7.1, OCH_2CH$_3$), 6.68 (1H, br, N*H*), 6.98–7.05 (2H, m, thienyl H_3 and H_5), 7.23–7.40 (2H, m, phenyl H_5 and H_4 + thienyl H_4), and 7.80–7.9 (2H, m, phenyl H_2 and H_6).

^{13}C NMR ($CDCl_3$): δ 14.3, 24.1, 26.4, 27.1, 28.7, 34.2, 36.0, 38.1, 39.8, 46.6 (br, *C*-B), 52.0, 60.8, 77.3, 84.9, 126.3, 127.0, 127.5, 127.7, 128.2, 128.4, 130.6, 130.7, 133.6, 140.7, 166.6, and 174.3.

EIMS: *m/z* 481 (62%, M^+), 436 (5%), 329 (14%), 302 (5%), 285 (8%), 245 (33%), 222 (9%), 178 (17%), 163 (11%), 135 (23%), 124 (33%), 107 (12.5%), 97 (100%), 84 (57%), 70 (15%), and 45 (18%).

Analytically calculated for $C_{26}H_{32}BNO_5S$: C, 64.87; H, 6.70; N, 2.91. Found: C, 64.77; H, 6.81; N, 2.83.

*(R)-(3-Carboxyphenyl)-(2-thiophen-2-yl-acetylamino)methaneboronic acid (−)-**2***—Compound (+)-**5** (270 mg, 0.56 mM) was treated with degassed HCl 3 M (13 ml) at 100 °C for 1 h under argon. The reaction mixture was extracted with diethyl ether (2 × 10 ml), and the aqueous phase was concentrated under reduced pressure to afford a solid residue, which was crystallized from a few milliliters of methanol/diethyl ether affording the desired inhibitor (−)-**2** as a whitish crystalline powder. mp, 245–247 °C dec, $[\alpha]_D$: −78.0 (*c* 0.4, CH_3OH). IR: *ν* 3398, 1704, and 1606.

^{1}H NMR (CD_3OD): δ 3.87 (1H, br s, C*H*-B), 4.18 (2H, s, CH_2-CO), 7.00–7.05 (1H, m, thienyl H_4), 7.13–7.14 (1H, m, thienyl H_3), 7.30–7.41 (3H, m, phenyl H_5 and H_6 + thienyl H_5), and 7.80 (2H, m, phenyl H_2 and H_4).

^{13}C NMR (CD_3OD): δ 31.0, 53.0 (br, *C*-B), 126.2, 127.0, 127.2, 127.4, 128.2, 128.4, 130.6, 130.8, 133.5, 141.5, 168.9, and 178.5.

Elemental analysis and EIMS of the free boronic acid were not obtainable (24).

TABLE 1

MIC values of *E. coli* DH10B containing SHV-1 and all 19 variants at Arg-244

244 Clone	Ampicillin	Ampicillin/clavulanate	Piperacillin	Cephalothin
	μg/ml	*μg/ml*	*μg/ml*	*μg/ml*
Arg (WT)[a]	**>16,384**	**50/2**	**2,048**	**64**
Ala	256	50/4	64	4
Asn	256	50/4	64	4
Asp	2	50/0.06	2	4
Cys[b]	128	50/2	64	4
Gln	**1,024**	**50/16**	**256**	**4**
Glu	**256**	**50/8**	**32**	**4**
Gly[b]	256	50/4	64	4
His[b]	1,024	50/8	128	4
Ile	256	50/8	32	4
Leu[b]	**128**	**50/16**	**32**	**4**
Lys	2,048	50/8	512	8
Met	512	50/16	64	4
Phe	256	50/8–16	32	4
Pro	1	50/0.06	2	4
Ser[b]	**1,024**	**50/8**	**128**	**4**
Thr[b]	512	50/8	64	4
Trp	8	50/0.06	4	4
Tyr	128	50/16	16	4
Val	128	50/8–16	16	4

[a] Bold font represents variants chosen for kinetic analysis.
[b] Substitutions found clinically in TEM.

Structure Analysis—Protein Data Bank (PDB)[7] coordinates of SHV-1 and TEM-1 were examined using ViewerLite® (Accelrys®, San Diego, CA). The following Research Collaboratory for Structural Bioinformatics PDB codes were analyzed: 1SHV (SHV-1) (25) and 1BTL (TEM-1) (26).

Molecular Representation—β-Lactam backbones were drawn with the Sketcher module in Insight II Version 2005 Molecular Modeling System (Accelrys®, SGI, Octane workstation IRIX 6.5.28). Molecules were built into three-dimensional structures with Converter, energy-minimized, and overlaid on their β-lactam rings. β-Lactams were positioned into the active site of SHV-1 (PDB 1SHV, see above), with only Arg-244, Thr-235, and Ser-70 visualized.

RESULTS

Mutagenesis and Immunoblotting—16 of 19 amino acid substitutions were obtained in the initial sequencing screen. $bla_{SHV\text{-}1(R244K)}$, $bla_{SHV\text{-}1(R244M)}$, and $bla_{SHV\text{-}1(R244F)}$ were constructed by site-directed mutagenesis. Full-length expression of all variants was confirmed by immunoblotting (data not shown).

Antibiotic Susceptibility—To test the effects of the single amino acid substitutions at Arg-244 on *in vivo* β-lactam susceptibility, MICs against all 19 variants were determined for ampicillin, ampicillin/clavulanate, piperacillin, and cephalothin in *E. coli* DH10B cells (Table 1). Twelve amino acid substitutions in SHV-1 increased the MIC values for the inhibitor combination ampicillin/clavulanate by at least two dilutions (from 50/2 to >50/8 μg/ml). MIC values for the penicillins (ampicillin and piperacillin) and the cephalosporin, cephalothin, were universally decreased.

[7] The atomic coordinates for the previously published crystal structures discussed in this report can be accessed through the Research Collaboratory for Structural Bioinformatics Protein Data Bank: 1SHV and 1BTL.

TABLE 2
Kinetic properties of SHV-1 and variants at Arg-244 for clavulanate, ampicillin, and nitrocefin

	SHV-1	R244S	R244Q	R244L	R244E
Clavulanate					
K_i (μM)	1 ± 0.04	63 ± 3	85 ± 7	360 ± 20	1000 ± 150
k_{inact} (s^{-1})	0.04 ± 0.002	0.09 ± 0.005	0.09 ± 0.007	0.11 ± 0.01	0.08 ± 0.008
k_{inact}/K_i ($\mu M^{-1}\ s^{-1}$)	0.04 ± 0.003	0.0014 ± 0.0001	0.0011 ± 0.0001	0.00031 ± 0.00003	0.00008 ± 0.00001
k_{cat}/k_{inact}	60 ± 10	50 ± 10	180 ± 10	550 ± 30	55 ± 10
k_{cat} (s^{-1})	2.4 ± 0.4	4.5 ± 0.9	19 ± 2	61 ± 6	4.4 ± 0.9
Ampicillin					
K_m (μM)	165 ± 10	255 ± 45	1190 ± 120	2240 ± 590	3500 ± 1800
k_{cat} (s^{-1})	3700 ± 400	390 ± 50	1400 ± 160	800 ± 170	115 ± 50
k_{cat}/K_m ($\mu M^{-1}\ s^{-1}$)	22 ± 3	1.5 ± 0.3	1.2 ± 0.2	0.4 ± 0.1	0.03 ± 0.02
Nitrocefin					
K_m (μM)	21 ± 3	55 ± 4	110 ± 9	590 ± 30	250 ± 10
k_{cat} (s^{-1})	290 ± 32	107 ± 11	270 ± 30	230 ± 20	20 ± 2
k_{cat}/K_m ($\mu M^{-1}\ s^{-1}$)	14 ± 2.5	2 ± 0.25	2.4 ± 0.3	0.4 ± 0.04	0.08 ± 0.009

Kinetic Behavior of Inhibitor Resistant β-Lactamases with Clavulanate—Susceptibility data served as a guide for selection of β-lactamases for further kinetic analysis. Four clavulanate-resistant enzymes were chosen: SHV R244S, R244Q, R244L, and R244E.

A common feature of the resistant enzymes is reduced affinity for clavulanate, with K_i values increasing 60- to 1000-fold (Table 2). Unexpectedly, the clavulanate-resistant enzymes exhibited increased k_{inact} values. This is in sharp contrast to the TEM enzymes, R244Q and R244T, which exhibited a 100-fold decrease in k_{inact} (14). At concentrations equal to the K_i for clavulanate, all SHV Arg-244 variants were rapidly inactivated (Fig. 4). This is again much different from the analysis of R244S, R244Q, and R244T TEM variants at Arg-244, which never achieve complete inactivation (14, 16).

Despite the increased rates of inactivation, the markedly decreased affinity of these mutant enzymes for clavulanate reduced the inactivation efficiency (k_{inact}/K_i) by 25- to 500-fold (Table 2). Thus, decreased affinity is the primary cause for resistance to inactivation by clavulanic acid.

In 24-h inactivation experiments, SHV-1, R244S, and R244E enzymes required approximately the same amount of clavulanate to achieve a 90% reduction in enzyme activity (k_{cat}/k_{inact}, or partition ratio) (Table 2). Alternatively, the R244Q and R244L enzymes exhibited a 3- to 9-fold increase in k_{cat}/k_{inact}, respectively. The derived k_{cat} values were increased for all mutants tested, most notably the R244Q and R244L mutants, and this enhanced ability to catalyze the turnover of inhibitor likely contributed to resistance.

Determining the Nature of the Intermediates: Electrospray Ionization MS with SHV-1 and R244S—Clavulanate undergoes a multistep reaction pathway (2). Candidate intermediates were observed previously for SHV-1 and S130G, also an inhibitor-resistant variant (Fig. 5) (2). Intact mass spectrometry was performed on SHV-1 and R244S to observe the covalent intermediates in the inactivation pathway. The R244S variant was chosen, because it is the most common mutant found in TEM at position 244.

As seen in Fig. 5, when SHV-1 and R244S were incubated with clavulanate, nearly identical covalent intermediates were formed. This includes, within experimental error, the Δ +52 adduct that is postulated to represent the terminally inactivated, cross-linked enzyme species, and the Δ +70, Δ +88, and

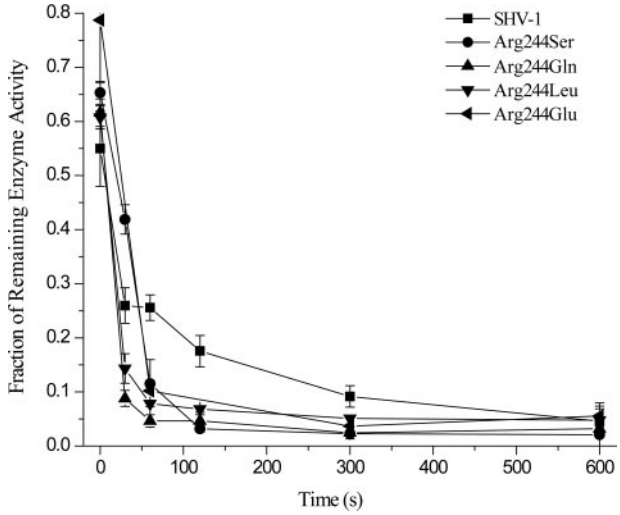

FIGURE 4. **Timed inactivation of SHV-1 and R244S, R244Q, R244L, and R244E.** Enzymes were incubated with K_i concentrations of clavulanate and initial velocities of nitrocefin hydrolysis measured at time points 0–600 s.

Δ +155 Da adducts previously observed in TEM-1 and SHV-1 (2, 27). The only differences between the two spectra include a Δ +175 adduct seen in only SHV-1 and a Δ +194 peak visualized in R244S only. The Δ +175 peak is very minor and may be hidden within the shoulder of the Δ +157 adduct of R244S. Alternatively, the Δ +194 peak in R244S could be a protein modification (oxidation), which shifted the Δ +175 adduct by +19.

Kinetic Behavior of Inhibitor Resistant Enzymes with β-Lactam Substrates—Kinetic parameters for SHV-1 and the inhibitor-resistant mutants R244S, R244Q, R244E, and R244L for ampicillin and nitrocefin are reported in Table 2. Affinity is reduced for all variants, with R244S and R244Q demonstrating the lowest K_m values. Interestingly, k_{cat} is universally reduced; the enzymes with the highest k_{cat}/k_{inact} values for clavulanate (R244Q and R244L) display the highest k_{cat} values for substrates among the Arg-244 variants. Catalytic efficiency (k_{cat}/K_m) of all variants was greatly reduced for ampicillin (14- to 700-fold) and nitrocefin (5- to 175-fold).

To assess the importance of the position of the C_{3-4} carboxylate in substrate affinity, we next tested piperacillin, cephalothin, and meropenem (Fig. 1). Because accurate hydrolysis of these substrates was difficult to measure for the Arg-244 vari-

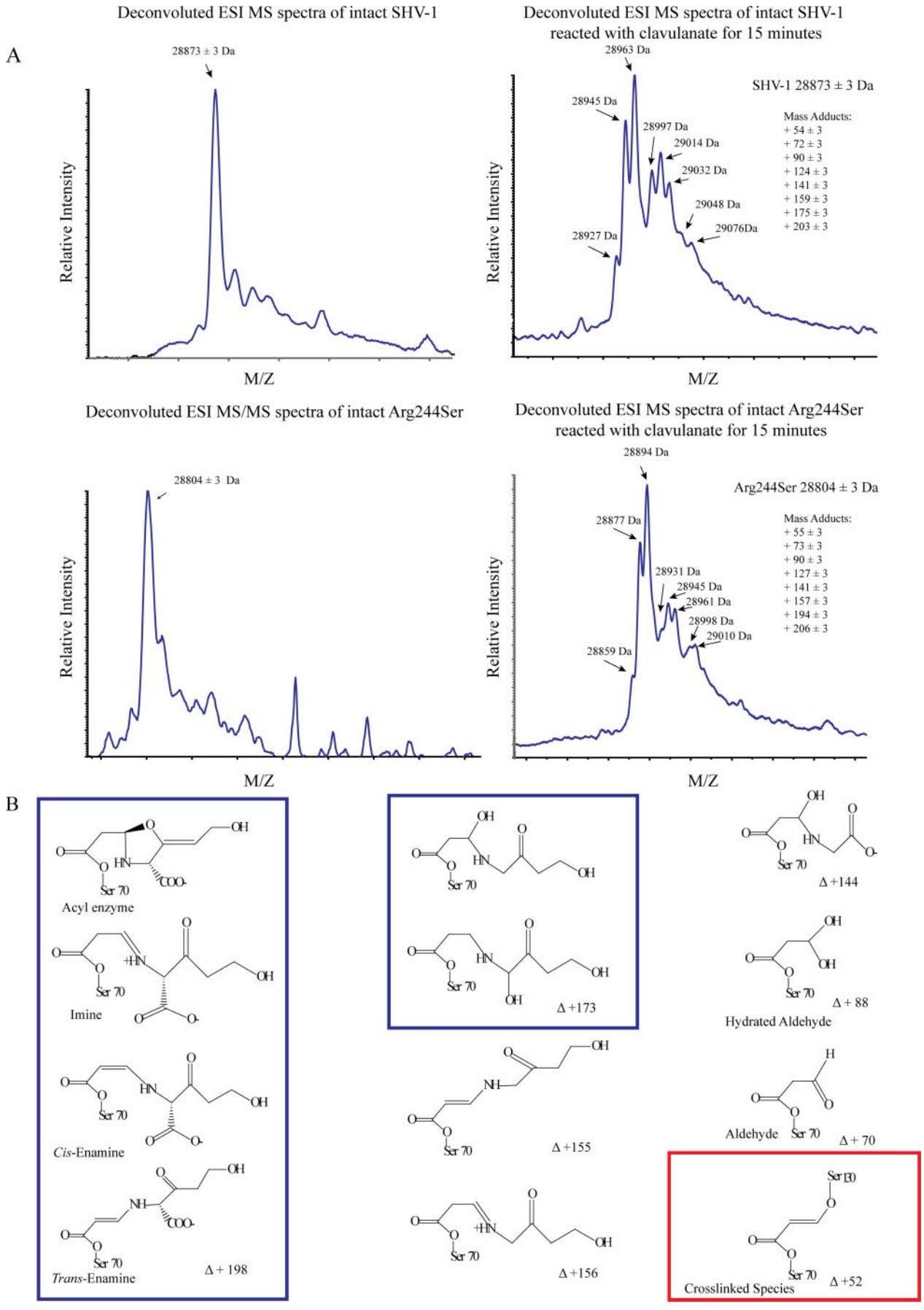
A
Deconvoluted ESI MS spectra of intact SHV-1
28873 ± 3 Da
Relative Intensity
M/Z
Deconvoluted ESI MS spectra of intact SHV-1 reacted with clavulanate for 15 minutes
28963 Da
28945 Da
28997 Da
29014 Da
29032 Da
29048 Da
29076Da
28927 Da
SHV-1 28873 ± 3 Da
Mass Adducts:
+ 54 ± 3
+ 72 ± 3
+ 90 ± 3
+ 124 ± 3
+ 141 ± 3
+ 159 ± 3
+ 175 ± 3
+ 203 ± 3
Relative Intensity
M/Z
Deconvoluted ESI MS/MS spectra of intact Arg244Ser
28804 ± 3 Da
Relative Intensity
M/Z
Deconvoluted ESI MS spectra of intact Arg244Ser reacted with clavulanate for 15 minutes
28894 Da
28877 Da
28931 Da
28945 Da
28961 Da
28998 Da
29010 Da
28859 Da
Arg244Ser 28804 ± 3 Da
Mass Adducts:
+ 55 ± 3
+ 73 ± 3
+ 90 ± 3
+ 127 ± 3
+ 141 ± 3
+ 157 ± 3
+ 194 ± 3
+ 206 ± 3
Relative Intensity
M/Z
B
Acyl enzyme
Imine
Cis-Enamine
Trans-Enamine
Δ + 198
Δ +173
Δ +155
Δ +156
Δ +144
Δ + 88
Hydrated Aldehyde
Aldehyde
Δ + 70
Crosslinked Species
Δ +52
Ser 70

TABLE 3
Dissociation constants of β-lactam substrates and boronic acid transition state inhibitors for SHV-1 and Arg-244 variants

	SHV-1	R244S	R244Q	R244L	R244E
	μM	μM	μM	μM	μM
Piperacillin (K_d)	66 ± 4	134 ± 5	860 ± 50	3,700 ± 400	12,000 ± 400
Cephalothin (K_d)	74 ± 4	2,000 ± 130	1,500 ± 30	22,000 ± 700	56,000 ± 5,000
Meropenem (K_d)	37 ± 2.5	15,200 ± 700	17,300 ± 700	102,000 ± 7,000	>100,000
Compound **1** (K_i)	30 ± 1	34 ± 2	30 ± 2	43 ± 3	116 ± 10
Compound **2** (K_i)	3.9 ± 0.3	24.3 ± 0.4	18.5 ± 0.7	71 ± 7	156 ± 15

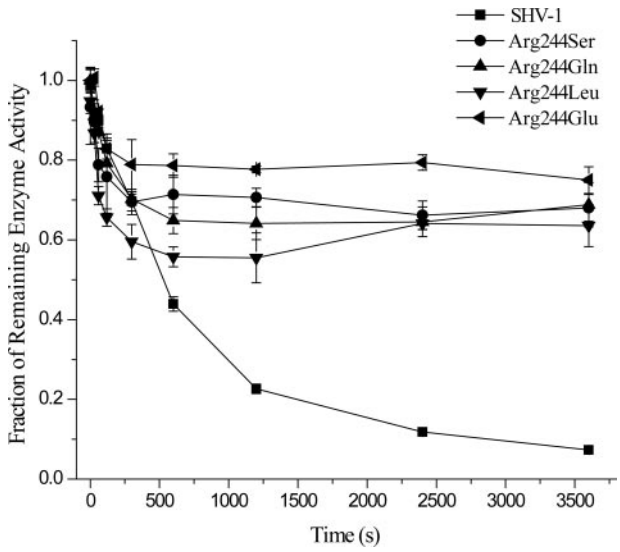

FIGURE 6. **The time-dependent inhibition of the chiral cephalothin boronic acid transition state inhibitor (compound 2) with SHV-1 and SHV R244S, R244Q, R244L, and R244E.** Enzymes were incubated with inhibitor at concentrations equal to the K_i, and initial velocities of nitrocefin hydrolysis were assessed at 0–3600 s. Initial K_i determination was performed after a 5-min incubation.

ants, affinity was assessed by competition reaction with the indicator substrate nitrocefin (Table 3). Again, all substitutions at position 244 resulted in enzymes with reduced affinities for these substrates (2- to 180-fold increase in K_d for piperacillin, 20- to 750-fold for cephalothin, and a striking 400- to >2700-fold for meropenem). As seen above, R244S and R244Q retained the highest affinities.

Probing the Active Site: Cephalothin Boronic Acid Transition State Analogs—Boronic acid analogs have been developed in recent years, both as high affinity inhibitors of β-lactamases and as probes to study reaction mechanism. They also serve to explore determinants of binding specificity (10, 11, 21, 22, 28). A majority of these compounds have been designed as achiral molecules containing the R1 side chains of penicillins and cephalosporins. Recently, chiral compounds have been developed to take advantage of affinity gains of the C_4 carboxylate (Fig. 1).

To investigate the importance of Arg-244 in SHV for coordination of the β-lactam carboxylate, we synthesized an achiral (compound **1**) and chiral (compound **2**) boronic acid derivative of cephalothin (Fig. 1). In particular, we reasoned that the molecular architecture of **2** would closely resemble the interactions displayed by the antibiotic cephalothin (the carboxylic moiety at C_4 included) with the β-lactamase.

As expected, compound **1** inhibits SHV-1 and R244S, R244Q, and R244L with similar affinities (Table 3). In contrast, the R244E enzyme demonstrated an ~4-fold reduction in affinity compared with wild type. Because this analog should not interact directly with residue 244, we submit that this difference suggests a rearrangement in the tertiary structure of this variant.

Testing the chiral boronic acid transition state inhibitor, compound **2**, there was a 7-fold enhanced affinity for SHV-1 compared with compound **1**. R244S and R244Q both showed only modest improvements in K_i of binding to the chiral compound (<2-fold), and 244Leu and R244E had reduced affinity for **2**, indicating an unfavorable interaction of the C_4 carboxylate.

As has been described for other β-lactamase families (10, 21), we observed time-dependent inhibition of compound **2**, which is in contrast to the fast on/fast off time-independent inhibition of other (including **1**) boronic acid compounds. To compare our analysis to others, we chose a 5-min preincubation for our studies (10, 11, 21). To ensure the suitability of the 5-min preincubation for reaching equilibrium, we used the K_i concentrations measured at 5 min to further study the time course of inhibition from 0 to 3600 s (60 min) (Fig. 6). Interestingly, although all the mutant enzymes did reach steady state by 5 min, SHV-1 was increasingly inhibited with time, resulting in near complete inhibition by the 3600-s time point. Therefore, the true steady-state K_i value for SHV-1 with the chiral inhibitor is likely much lower than the 5-min measurement of 3.8 μM.

DISCUSSION

We show that many substitutions at Ambler position 244 in SHV produce the inhibitor-resistant phenotype. However, kinetic analysis of selected variants suggests that the demonstration of resistance to clavulanate in SHV is unique. The principal characteristic of resistance in SHV variants at Arg-244 is a reduction in affinity for the inhibitor. This property is shared by both TEM and SHV. However, unlike TEM, SHV mutants at position 244 do not demonstrate a reduction in k_{inact}. These inhibitor-resistant β-lactamases undergo rapid inactivation with clavulanate provided adequate inhibitor concentrations are achieved. Interestingly, both the inhibitor-susceptible and

FIGURE 5. *A*, deconvoluted mass spectra of SHV-1 and R244S before and after 15-min incubation with clavulanate. Spectra were obtained on a Q-STAR XL quadrupole-time-of-flight mass spectrometer equipped with a nanospray source. Eight distinct mass shifts were identified with both enzymes. *B*, proposed intermediates in the clavulanate inactivation pathway. The 198- and 173-Da adducts are represented by more than one candidate structure (*blue*). The terminally inactivated 52-Da cross-linked species is highlighted in *red* (2).

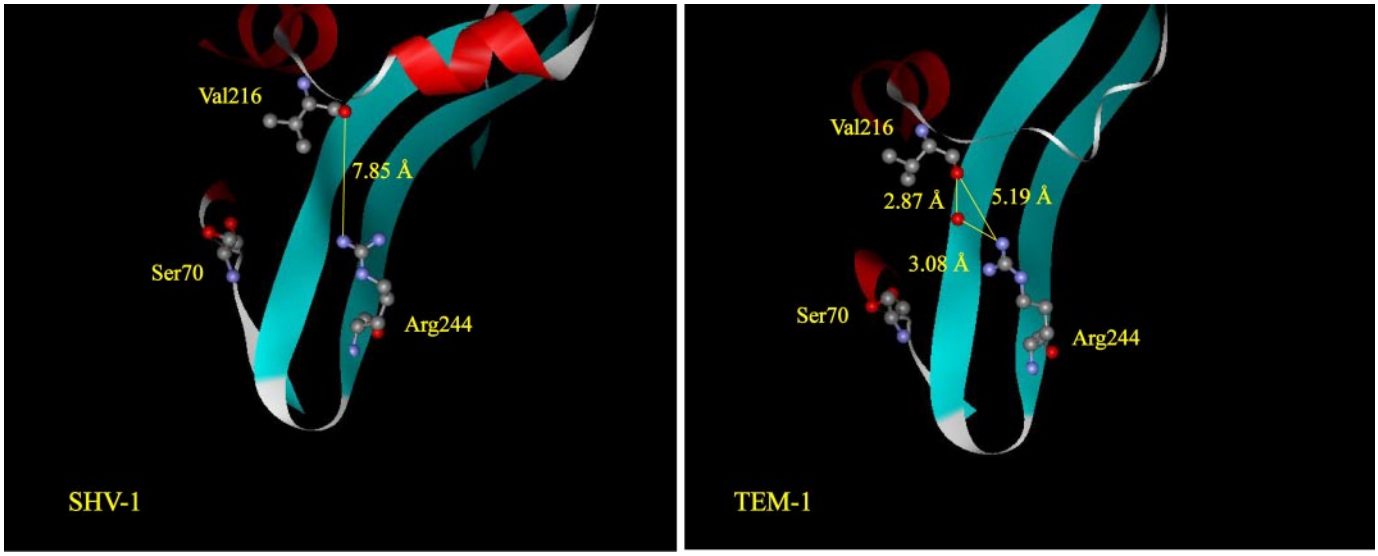

FIGURE 7. **Arg-244 in relation to Val-216 in the SHV-1 (1SHV) and TEM-1 (1BTL) in apo-enzyme crystal structure representations.** The distance between the backbone carbonyl oxygen of Val-216 and the nearest guanidinium nitrogen in SHV is 7.85 Å. In contrast, the distance in TEM-1 is 5.19 Å. Shown in TEM-1 is the bridging water molecule, which makes hydrogen bonds with Val-216 (2.87 Å) and Arg-244 (3.08 Å). The active site Ser-70 is shown for reference.

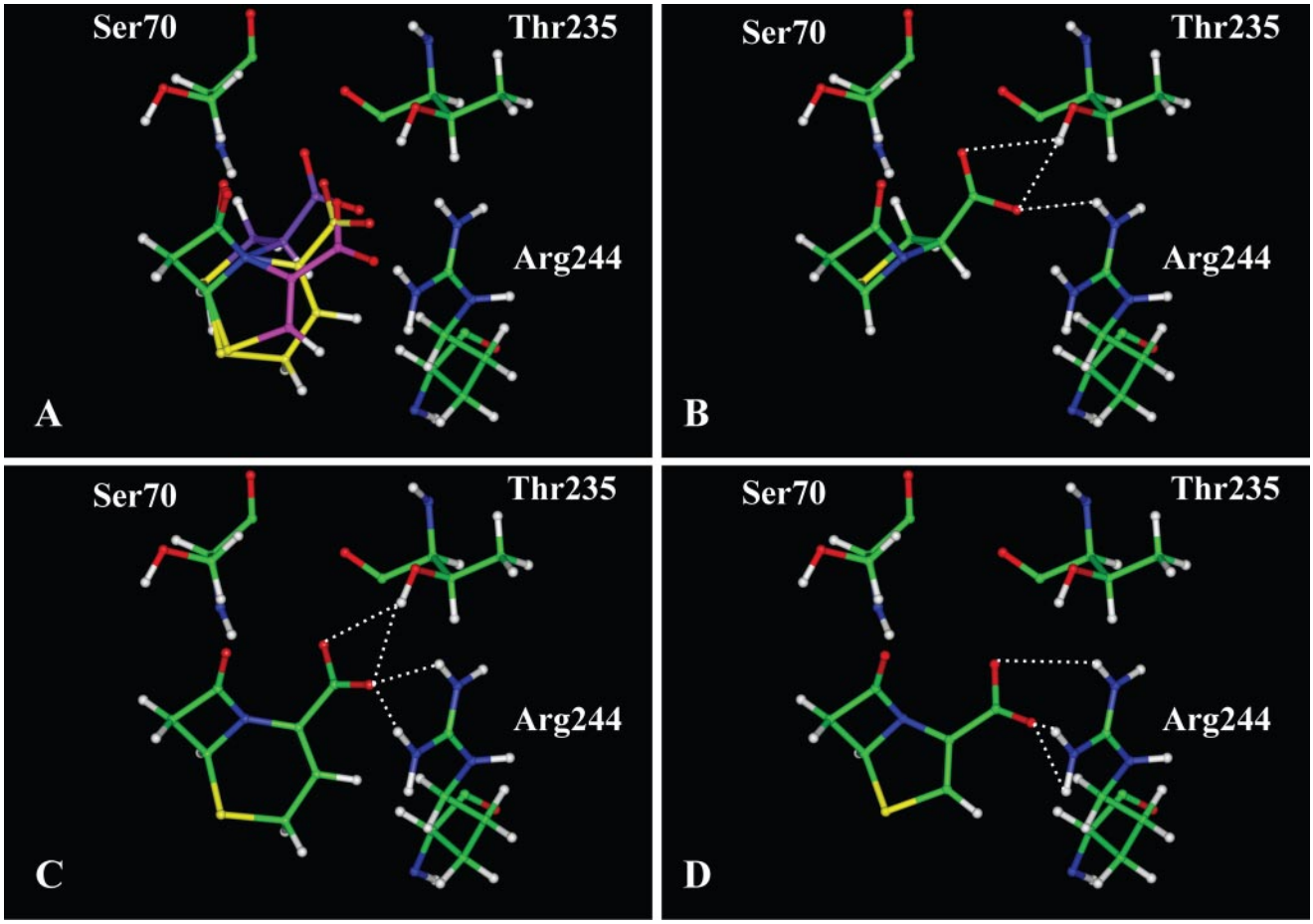

FIGURE 8. **Suggested role of Arg-244 in stabilizing the β-lactam carboxylate of penicillins, cephalosporins, and carbapenems.** The ring structures of ampicillin (*purple*), cephalothin (*yellow*), and meropenem (*pink*) were drawn using Sketcher (Accelrys®) and energy-minimized. The three structures were overlaid on the β-lactam ring, and the proposed orientation in the active site is shown (*A*). The penicillin (*B*), cephalosporin (*C*), and carbapenem (*D*) ring structures are depicted in relation to Arg-244 and Thr-235 (catalytic Ser-70 is shown for reference). The proposed bonding interactions are drawn in *white*.

inhibitor-resistant SHV enzymes follow the same reaction pathway; the products of inactivation of SHV-1 and R244S by clavulanate, as determined by mass spectrometry, are identical.

What accounts for this key difference in behavior between the TEM and SHV β-lactamases? We answer this question by examining the atomic structures of TEM-1, SHV-1, and the

SHV S130G variant. Examining a representation created from the PDB coordinates available for the TEM-1 apo-enzyme, a water molecule is clearly positioned between Arg-244 and the backbone carbonyl of Val-216 (Figs. 2 and 7) (10). One explanation for the catalytic deficit in TEM mutants at position 244 is displacement of that water molecule, which is essential for secondary clavulanate ring opening in the inactivation pathway. Comparing the apo-enzyme crystal structures of TEM-1 (26) and SHV-1 (25), the distances between the closest guanidinium nitrogen of Arg-244 and the backbone carbonyl oxygen Val-216 are significantly different (Fig. 7). For TEM, this distance is 5.19 Å, whereas in SHV the distance is 7.85 Å, a large distance for coordination of a water molecule. Therefore it is likely that, in SHV, protonation of the inhibitor is achieved by either a coordinated water molecule elsewhere in the active site, or from bulk water in the medium. Thus, substitutions at position 244 in SHV affect affinity but do not retard inhibitor turnover. This explanation is reminiscent of the observations made in the determination of the S130G apo-enzyme structure. In S130G the catalytic water molecule is only evident as the inhibitor is bound (29). Our data support the general hypothesis that the active site of inhibitor-resistant SHV enzymes is rehydrated. This raises the possibility that, despite different mutations, inhibitor-resistant SHV enzymes follow a common pathway to inactivation.

Studying the dissociation constants of penicillins, cephalosporins, and carbapenems provided us deeper insight into the reliance of Arg-244 binding to the different spatial positions of the C_{3-4} carboxylate and its role in catalysis (Fig. 8).

First, affinity for the penicillins is the least affected by substitutions at Arg-244. The carboxylate in this case is hanging from the sp^3-hybridized and *S*-configured C_3 carbon. In our model, it is likely that Arg-244 contributes one or two weak hydrogen bonds to the carboxylate in the Michaelis complex, with additional hydrogen bonding interactions coming from other residues in the binding pocket (Fig. 8*B*). For this reason, most inhibitor-resistant variants at Arg-244 in SHV retain weak penicillinase activity, and their emergence in the context of current β-lactam/β-lactamase inhibitor combinations, which utilize penicillins, is not excluded.

Second, the reductions in affinity are at the very least 20-fold (SHV R244Q) for cephalothin. Different from penicillins, the cephalosporin carboxylate is directly linked to the C_4 sp^2-hybridized carbon of the six-membered ring and, therefore, coplanar with C_3–C_4, with reduced rotational freedom due to conjugation. This likely brings the carboxylate in closer approximation to Arg-244 (Fig. 8*C*). The dramatic loss of cephalosporinase activity among Arg-244 variants shows that clavulanate-resistant variants that arise in the clinic would be susceptible to treatment with cephalosporins. That being said, excessive use of cephalosporins in the clinical setting may mask the emergence of inhibitor-resistant SHV enzymes.

Most revealing is our data for meropenem affinity. Like clavulanate, carbapenems act as very effective covalent inhibitors of class A β-lactamases.[8] Interestingly, replacement of Arg-244 results in total loss of affinity for meropenem. All of the mutants bound meropenem with millimolar affinity, and two of them (R244E and R244L) had K_d values >100 mM. This indicates that the carboxylate linked to the C_3 sp^2-hybridized carbon of the five-membered ring makes several crucial hydrogen bonding interactions with the guanidinium group of Arg-244 (Fig. 8*D*). Caution should be taken in the development of future inhibitors with planar C_3 carboxylates, because substitutions at residue 244 could seriously compromise their activity.

Last, we studied two boronic acid transition state analogs to further probe the contributions of Arg-244 variants to β-lactam carboxylate affinity. The achiral cephalothin boronic acid compound **1** contains just the R1 side chain of cephalothin. In contrast, the chiral cephalothin analog **2** more closely imitates the interactions of the natural substrate by the addition of a C_4 carboxylate on a phenyl ring (Fig. 1). Comparing affinity of both compounds allowed us to determine the extent to which each substitution of the β-lactamase affects binding to the carboxylate independently.

Against SHV-1, compound **2** demonstrates significantly greater affinity for the active site (nearly a log fold) compared with compound **1**. We observed that the R244S substitution at 244 has a modest, 40% increase in binding to **2** *versus* **1** (24 μM *versus* 34 μM). This supports our claim (see above) that there is another residue in the binding pocket that contributes to binding of the carboxylate, possibly Thr-235 (16). Alternatively, hydrophobic interactions with the phenyl ring of compound **2** could stabilize the inhibitor.

Compared with R244S, a slightly higher affinity is seen with R244Q (60% increase) for compound **2**, which may imply that the Gln residue itself is able to weakly interact with the inhibitor carboxylate. On the other hand, increased K_i values for **2** with R244L and R244E suggest unfavorable interactions with the inhibitor carboxylate and explain the drastic affinity reductions for β-lactams.

The differences in the time-dependent inactivation of compound **2** between the wild-type and mutant enzymes also provided a window into the importance of Arg-244 for turnover of substrate. The chiral compound **2** has been shown in crystal structures with TEM, CTX-M, and AmpC-type β-lactamases to assume the deacylation transition state (10, 21, 22). In TEM, although no structural rearrangements were seen upon binding to the inhibitor, there was movement of catalytic water molecules and a rearrangement of the inhibitor (10). If this reorganization is responsible for the time-dependent binding of compound **2** to SHV-1, the reduction in time dependence among the Arg-244 mutants may indicate a novel substrate deacylation role for Arg-244 (Fig. 6). Ongoing studies to determine the microscopic rate constants k_2 and k_3 of SHV variants at Arg-244 using stopped-flow kinetics will provide evidence for this role. Co-crystallization of SHV-1 and Arg-244 variants with the cephalothin transition state analogs are in progress.

In conclusion, we present evidence that TEM and SHV are different in their intrinsic binding and turnover of inhibitors (12). Despite similarities in sequence and phenotype between TEM and SHV, the kinetic differences revealed herein suggest that these two class A β-lactamases follow unique pathways in response to antibiotic pressure (an argument that would have

[8] M. Nukaga, C. R. Bethel, J. M. Thomson, J. R. Knox, and R. A. Bonomo, manuscript in preparation.

significant implications for the comparative study of penicillin-inactivating enzymes among prokaryotes). Awareness of the subtle yet mechanistically important differences in inactivation chemistry among class A β-lactamases could prove crucial in the future development of β-lactamase inhibitors.

Acknowledgments—Special thanks to Dr. Charles Hoppel for assistance with mass spectrometry, Magdalena Taracila for assistance with molecular modeling, and to Dr. Marion S. Helfand and Andrea M. Hujer for careful review of the manuscript.

REFERENCES

1. Thomson, J. M., and Bonomo, R. A. (2005) *Curr. Opin. Microbiol.* **8,** 518–524
2. Sulton, D., Pagan-Rodriguez, D., Zhou, X., Liu, Y., Hujer, A. M., Bethel, C. R., Helfand, M. S., Thomson, J. M., Anderson, V. E., Buynak, J. D., Ng, L. M., and Bonomo, R. A. (2005) *J. Biol. Chem.* **280,** 35528–35536
3. Pagan-Rodriguez, D., Zhou, X., Simmons, R., Bethel, C. R., Hujer, A. M., Helfand, M. S., Jin, Z., Guo, B., Anderson, V. E., Ng, L. M., and Bonomo, R. A. (2004) *J. Biol. Chem.* **279,** 19494–19501
4. Helfand, M. S., Totir, M. A., Carey, M. P., Hujer, A. M., Bonomo, R. A., and Carey, P. R. (2003) *Biochemistry* **42,** 13386–13392
5. Zhou, X. Y., Bordon, F., Sirot, D., Kitzis, M. D., and Gutmann, L. (1994) *Antimicrob. Agents Chemother.* **38,** 1085–1089
6. Imtiaz, U., Manavathu, E. K., Mobashery, S., and Lerner, S. A. (1994) *Antimicrob. Agents Chemother.* **38,** 1134–1139
7. Blazquez, J., Baquero, M. R., Canton, R., Alos, I., and Baquero, F. (1993) *Antimicrob. Agents Chemother.* **37,** 2059–2063
8. Buynak, J. D. (2004) *Curr. Med. Chem.* **11,** 1951–1964
9. Weiss, W. J., Petersen, P. J., Murphy, T. M., Tardio, L., Yang, Y., Bradford, P. A., Venkatesan, A. M., Abe, T., Isoda, T., Mihira, A., Ushirogochi, H., Takasake, T., Projan, S., O'Connell, J., and Mansour, T. S. (2004) *Antimicrob. Agents Chemother.* **48,** 4589–4596
10. Wang, X., Minasov, G., Blazquez, J., Caselli, E., Prati, F., and Shoichet, B. K. (2003) *Biochemistry* **42,** 8434–8444
11. Morandi, F., Caselli, E., Morandi, S., Focia, P. J., Blazquez, J., Shoichet, B. K., and Prati, F. (2003) *J. Am. Chem. Soc.* **125,** 685–695
12. Knox, J. R. (1995) *Antimicrob. Agents Chemother.* **39,** 2593–2601
13. Ambler, R. P., Coulson, A. F., Frere, J. M., Ghuysen, J. M., Joris, B., Forsman, M., Levesque, R. C., Tiraby, G., and Waley, S. G. (1991) *Biochem. J.* **276,** 269–270
14. Delaire, M., Labia, R., Samama, J. P., and Masson, J. M. (1992) *J. Biol. Chem.* **267,** 20600–20606
15. Zafaralla, G., Manavathu, E. K., Lerner, S. A., and Mobashery, S. (1992) *Biochemistry* **31,** 3847–3852
16. Imtiaz, U., Billings, E., Knox, J. R., Manavathu, E. K., Lerner, S. A., and Mobashery, S. (1993) *J. Am. Chem. Soc.* **115,** 4435–4442
17. Rice, L. B., Carias, L. L., Hujer, A. M., Bonafede, M., Hutton, R., Hoyen, C., and Bonomo, R. A. (2000) *Antimicrob. Agents Chemother.* **44,** 362–367
18. Hujer, A. M., Hujer, K. M., Helfand, M. S., Anderson, V. E., and Bonomo, R. A. (2002) *Antimicrob. Agents Chemother.* **46,** 3971–3977
19. Lin, S., Thomas, M., Shlaes, D. M., Rudin, S. D., Knox, J. R., Anderson, V., and Bonomo, R. A. (1998) *Biochem. J.* **333,** 395–400
20. Cheng, Y., and Prusoff, W. H. (1973) *Biochem. Pharmacol.* **22,** 3099–3108
21. Chen, Y., Shoichet, B., and Bonnet, R. (2005) *J. Am. Chem. Soc.* **127,** 5423–5434
22. Chen, Y., Minasov, G., Roth, T. A., Prati, F., and Shoichet, B. K. (2006) *J. Am. Chem. Soc.* **128,** 2970–2976
23. Caselli, E., Powers, R. A., Blasczcak, L. C., Wu, C. Y., Prati, F., and Shoichet, B. K. (2001) *Chem. Biol.* **8,** 17–31
24. Hall, D. G. (2005) in *Boronic Acids: Preparation and Applications in Organic Synthesis and Medicine*, First Ed. (Hall, D. G., Ed.) pp. 7–14, Wiley-VCH, Weinheim
25. Kuzin, A. P., Nukaga, M., Nukaga, Y., Hujer, A. M., Bonomo, R. A., and Knox, J. R. (1999) *Biochemistry* **38,** 5720–5727
26. Jelsch, C., Mourey, L., Masson, J. M., and Samama, J. P. (1993) *Proteins* **16,** 364–383
27. Brown, R. P., Aplin, R. T., and Schofield, C. J. (1996) *Biochemistry* **35,** 12421–12432
28. Powers, R. A., Caselli, E., Focia, P. J., Prati, F., and Shoichet, B. K. (2001) *Biochemistry* **40,** 9207–9214
29. Sun, T., Bethel, C. R., Bonomo, R. A., and Knox, J. R. (2004) *Biochemistry* **43,** 14111–14117